Available online at www.sciencedirect.com
ScienceDirect
Journal of the European Ceramic Society 29 (2009) 465–472
www.elsevier.com/locate/jeurceramsoc

The role of carbon biotemplate density in mechanical properties of biomorphic SiC

N.R. Calderon [a,b,*], M. Martinez-Escandell [a,b], J. Narciso [a,b], F. Rodríguez-Reinoso [a,b]

[a] *Departamento de Química Inorgánica, Universidad de Alicante, Apdo. 99, 03080 Alicante, Spain*
[b] *Instituto Universitario de Materiales de Alicante (IUMA), Apdo. 99, 03080 Alicante, Spain*

Received 22 November 2007; received in revised form 27 May 2008; accepted 30 May 2008
Available online 8 August 2008

Abstract

Biomorphic SiC was prepared from four types of Mediterranean wood as carbon precursor. Carbon biotemplates were obtained by pyrolysis and carbonization up to 1400 °C and they were infiltrated with liquid silicon in two different directions. A linear correlation between bending strength and bioSiC density for different types of softwood and hardwood has been found. Mechanical properties were modelled according to the MSA (minimum solid area) approach. Fairly good correlation was found when biomorphic SiC is treated as porous solid. Moreover, the fabrication of bioSiC from carbon biotemplates heat-treated up to 2500 °C has been additionally studied. An improvement up to 56% in flexural strength has been reached by densification of bioC at such high temperature.

Keywords: Microstructure; Mechanical properties; Thermal expansion; SiC; Reactive infiltration

1. Introduction

Recently, ceramics mimicking the biological structure of natural developed tissues have attracted increasing interest.[1–3] The lightweight and open porosity of these materials make them great candidates for structural applications in biomedicine[4] and also at high temperature.[5] Several research groups have developed biotemplating high temperature techniques to convert biological structures into ceramic materials. Thus, different kinds of wood have been converted into Si/SiC composites by reactive infiltration with liquid silicon[6–10] whereas Si-vapour phase infiltration[11–13] and carbothermal reduction reaction[14] have been used to make different porous SiC ceramics. Detailed mechanical tests and microstructural characterization have shown some outstanding mechanical properties of biomorphic SiC.[6,8–10,15–20] However, high scatter of results is found in SiC properties produced from natural substrates. This fact is commonly attributed to the different pore structure and anisotropy of each precursor, the term pore structure being generally admitted to be in this case the shape, size and distribution of tracheidal cells (in softwood) and vessels (in hardwood).

The aim of this work is to demonstrate that SiC mechanical properties produced from wood follow a general trend which is mainly a function of SiC density and not so dependent on precursor pore structure. Therefore, four wood species with different pore morphology and covering a wide range of porosity were selected as carbon precursors to produce SiC ceramics by reactive infiltration with liquid silicon. The effect of high temperature treatment on carbon substrate and its influence on ceramic properties was additionally studied.

2. Experimental procedure

2.1. Precursor materials

Four different kinds of wood, two softwood and two hardwood, covering a range of density and pore structure were selected to produce bioSiC. Typical Mediterranean species from local sources were used due to their availability and low cost. Chosen wood species were: pine (*Pinus pinea*), cedar (*Cedrela odorata*), almond (*Prunus amygdalus*) and olive (*Olea europaea*) wood, in increasing order of density and hardness. Wood materials were cut into 10 mm × 10 mm × 50 mm rectangular bars parallel to the axial direction. A minimum of five

* Corresponding author at: Departamento de Química Inorgánica, Universidad de Alicante, Apdo. 99, 03080 Alicante, Spain.
E-mail address: noelia.rojo@ua.es (N.R. Calderon).

0955-2219/$ – see front matter © 2008 Elsevier Ltd. All rights reserved.
doi:10.1016/j.jeurceramsoc.2008.05.049

preforms of each type of wood were processed for each set of experimental conditions.

2.2. Fabrication method

Wood preforms were dried for 24 h at 100 °C in an oven and then pyrolyzed under nitrogen at 1 MPa in a pressurized stainless steel reactor, heated by a sand-fluidized bed furnace. A slow heating rate of 1 °C/min was applied up to 520 °C. Thereafter, pyrolyzed wood preforms were further carbonized in a horizontal furnace up to 1400 °C during 60 min, using an argon flow of 60 ml/min and a heating rate of 1 °C/min up to the peak temperature. Some of the carbonized preforms were further heat-treated up to 2500 °C into a high temperature furnace using an argon flow and a heating rate of 10 °C/min (at Schunk Kohlenstofftechnik GmbH in Heuchelheim, Germany). The final carbon preforms were ready to be used directly as template structures to produce bioSiC with tailored porosity. Ceramization was performed in a horizontal furnace by reactive infiltration with liquid silicon (Silicon lumps, Aldrich, purity 98.5 wt%) at 1450 °C for 180 min using an argon flow of 60 ml/min.

2.3. Density and porosity measurement

Geometrical density of bioC and bioSiC was determined by measuring weight and volume of the specimens. Bulk density and open porosity were measured by Archimedes' method in water (standard DIN 51918), employing an AG204 delta range analytical balance and the Density Kit AG from Mettler Toledo. Skeleton and powder densities were measured by helium pycnometry (AccuPyc 1330TC, Micromeritics). Powder materials were obtained from preforms by grinding in a ball mill (S100, Retsch). Open and closed porosity values were obtained from the relationship between geometrical, skeleton and powder density of the materials.

2.4. Crystal structure

Crystal structure of reaction products was determined by X-ray diffraction (XRD) employing an X-ray diffractometer Bruker model D8 advance, fitted with a Cu cathode and Ni filter, using Bragg–Brentano geometry and monochromated Cu $K\alpha_1$ radiation ($\lambda = 1.5406$ Å). The device operated at 40 kV and 40 mA, and for measurements a step of 0.1° and a preset time of 3 s were used in the angular scanning from 10° to 80°. To overcome the non-planarity of samples, and work properly with parallel optical beam, a Göbel mirror was used.

2.5. Microstructure

Microstructure of both bioC and bioSiC was analyzed by scanning electron microscopy (SEM) using a Hitachi microscope model S-3000N. Energy dispersive X-ray analysis (EDX) Link QK 200 was used to identify the chemical composition of different phases of the materials. Samples were coated with a gold thin layer to enhance the electronic conductivity.

2.6. Thermogravimetric analysis

Simultaneous thermogravimetric differential analysis was carried out on a SDT 2960 simultaneous DSC–TGA from TA Instruments. Pure α-alumina powder (10 mg) was used as reference and 10-mg wood pieces were placed in the open alumina cell. TGA–DTA measurements were carried out using a heating rate of 5 °C/min up to 900 °C with a nitrogen flow of 100 ml/min.

2.7. Mechanical properties

Three-point bending strength of bioSiC was determined at room temperature using an Instron 4411 universal testing machine. Mechanical tests were carried out following standard DIN IEC 413 using specimens of 4 mm × 8 mm × 32 mm, 26 mm of span length and a crosshead displacement rate of 0.1 mm/min. Young's modulus and strain-to-failure values were calculated from the linear zone of stress–strain curves.

2.8. Thermal properties

The coefficient of thermal expansion (CTE) for bioSiC was calculated from the expansion curves of the material following the ASTME 831-86 standard. The device employed was a TMA 2940 thermomechanical analyzer from TA Instruments. Specimen size was 5 mm × 5 mm × 10 mm. Samples were submitted to four cycles of heating up to 500 °C and cooling down to 50 °C, at 3 °C/min rate, and isothermal stages of 5 min at maximum and minimum temperatures. Applied force was 0.05 N and a nitrogen flow of 150 ml/min was supplied.

3. Results and discussion

3.1. Carbon biotemplates

3.1.1. Thermogravimetric analysis

Characterization of the thermal degradation of wood under nitrogen was performed using thermogravimetric analysis (TG) at atmospheric pressure. TG curves for the different woods are plotted on the same graph for comparison and shown in Fig. 1. In general terms, there is an initial weight loss at 50–150 °C (a), where moisture is removed. Second step in the weight loss process occurs between 150 and 300 °C (b), which can be assigned to the decomposition of hemicellulose and release of small molecules such as CO, CO_2 and volatile components. At higher temperature range, 300–350 °C (c) weight loss occurs due to the decomposition of cellulose and lignin, which are higher molecular weight components, leaving behind the carbon structure.[7] Between 350 and 900 °C (d) weight loss occurs due to carbonization process, where carbon polymeric chains are cracked and graphene layers formed. As can be seen, some differences exist in the thermal behaviour of the four woods. These can be attributed to the different cell wall structure of each type of wood which limits the transformation rate of the reactions described above.[9] Carbon yield obtained from the different wood samples by TG at 900 °C ranged from 13 wt% (for pine) to 30 wt% (for olive), the data for 520 °C – the temperature

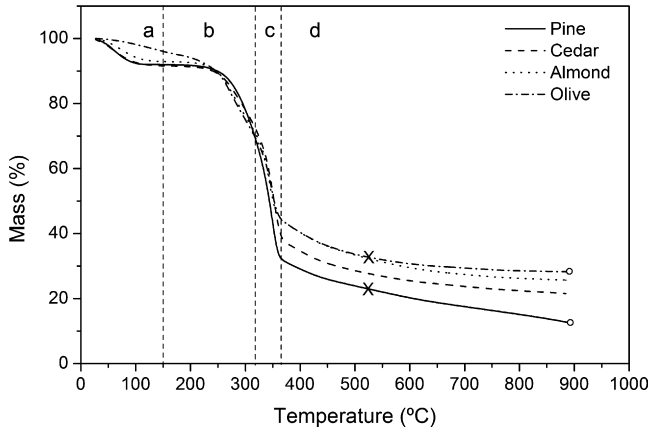

Fig. 1. Thermogravimetric curves for the selected woods in flowing nitrogen atmosphere. Carbon yield obtained from the different wood samples by TG at 900 °C (◯) and at 520 °C (×).

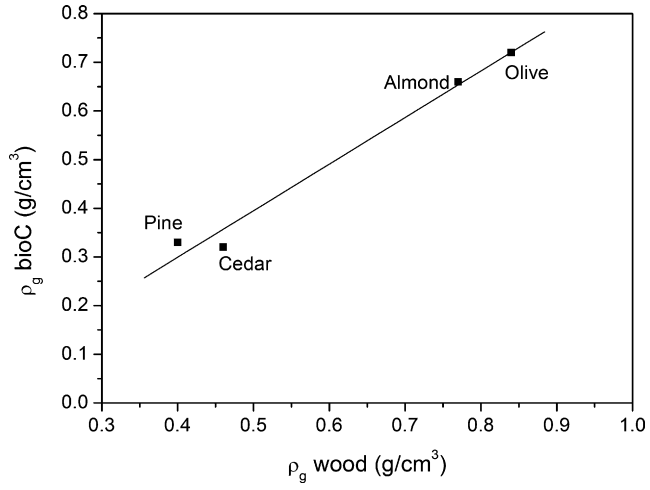

Fig. 2. Linear relationship obtained between wood geometrical density ($\rho_g$wood) and bioC geometrical density ($\rho_g$bioC) after carbonization process at 1400 °C.

used for 1 MPa pyrolysis of wood preforms – being 23 wt% (for pine) and 33 wt% (for olive).

3.1.2. Density and porosity

After pyrolysis up to 520 °C at 1 MPa, carbon yield of wood samples was 35–40 wt%, somewhat higher than the results obtained by atmospheric TG since pressure restricts the loss of volatile matter. The yield of bioC produced at 1400 °C (bioC-1400) is 30–35 wt% with a volume reduction up to 60% and a density decrease between 20% and 40% in respect to initial wood values.

Table 1 shows the average values of density for the original wood and corresponding bioC-1400 samples together with the open and closed porosity values for the latter. Four different types of carbon biotemplates have been obtained with very different pore structures, ranging from a really lightweight carbon material of 0.34 g/cm^3 with mainly open porosity (73%), derived from pine wood, to a heavier carbon material of 0.67 g/cm^3 with predominance of closed porosity (32%), derived from olive wood.

Fig. 2 shows that there is a linear relationship between the density of original wood and final bioC-1400, thus indicating that the initial chemical composition of the precursor seems to be of less or no significance.[21] Thermal degradation process of lignocellulosic material is not apparently related to the chemical composition and pore structure of each precursor species; it mainly depends on the wood density.[22]

3.2. Biomorphic SiC-based ceramics

BioC-1400 preforms obtained from the four woods were infiltrated with liquid silicon in two different directions, the axial direction (parallel to fibres and orientation of channels) and the radial direction (perpendicular to fibre orientation). The amount of silicon added for infiltration was just 10 wt% higher than the stoichiometry to ensure that enough Si is available for complete infiltration and to limit the amount of free silicon trapped into the pores. No attempt was done to remove the excess of silicon in order to compare the data with other published results obtained in the same fashion.

3.2.1. XRD analysis

Infiltrated samples were cut parallel to the infiltration direction and the reaction products were analyzed by XRD. All bioSiCs showed similar spectra. As a typical example, Fig. 3 includes the XRD profiles for cedar samples infiltrated in axial and radial directions. In both figures, peaks belonging to β-SiC and Si were found. However, a larger development of the SiC peaks is observed for the sample infiltrated in the axial direction. In contrast, X-ray diffractograms for samples infiltrated in the radial direction showed a larger development of the Si peaks. This means that the axial is the preferential infiltration direction since there is higher reactant consumption and SiC conversion.

Table 1
Average density of original woods (dry basis) and carbonized performs up to 1400 °C (bioC-1400) and up to 2500 °C (bioC-2500)

	Wood	bioC-1400			bioC-2500		
	ρ_g (g/cm^3)	ρ_g (g/cm^3)	P_{closed} (%)	P_{open} (%)	ρ_g (g/cm^3)	P_{closed} (%)	P_{open} (%)
Pine	0.40	0.34	7	73	–	–	–
Cedar	0.46	0.31	26	52	–	–	–
Almond	0.77	0.65	19	33	0.73	24	23
Olive	0.84	0.67	32	13	0.72	35	14

ρ_g: geometrical density, P_{closed}: closed porosity volume fraction, P_{open}: open porosity volume fraction.

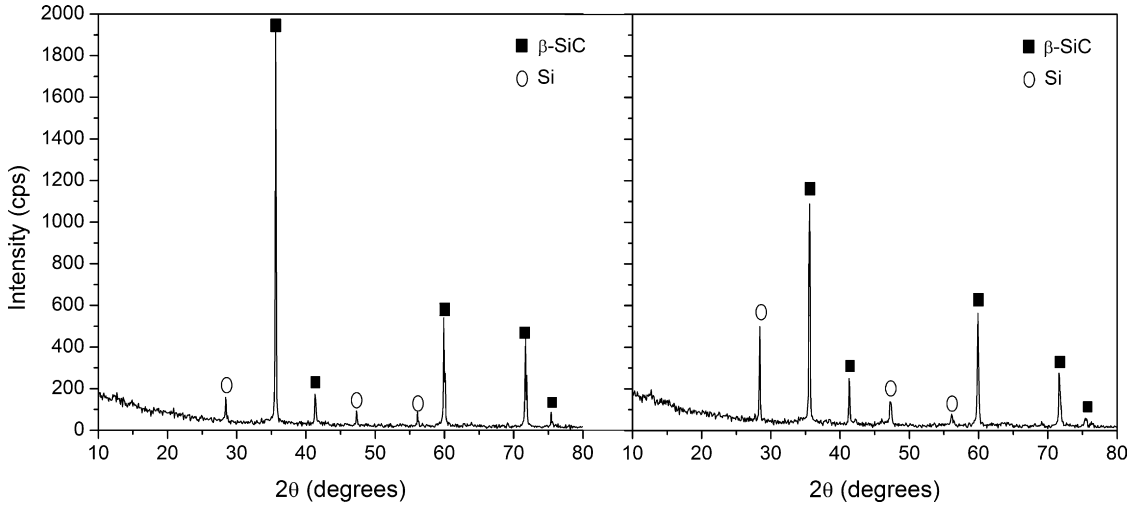

Fig. 3. X-ray diffraction profiles of the cedar carbon preform infiltrated in (a) axial direction and (b) radial direction.

3.2.2. *Microstructure*

BioSiC microstructure was observed by SEM. Figs. 4 and 5 show the microstructure of bioSiCs derived from pine and almond wood, respectively. BioSiCs are anisotropic, with a highly connected pore microstructure which is a consequence of being mimetic to the carbon biotemplate and hence to the original wood.[20] BioSiC derived from pine wood (Fig. 4) shows a typical softwood microstructure, composed by open pores with

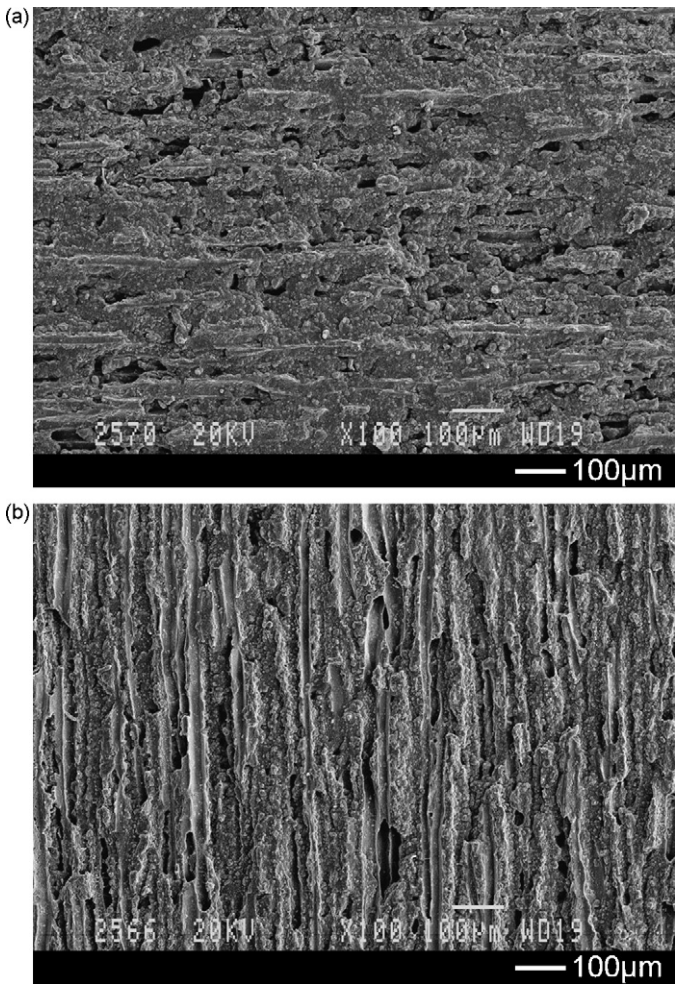

Fig. 4. SEM micrographs of biomorphic SiC derived from pine wood infiltrated in (a) radial section and (b) axial section.

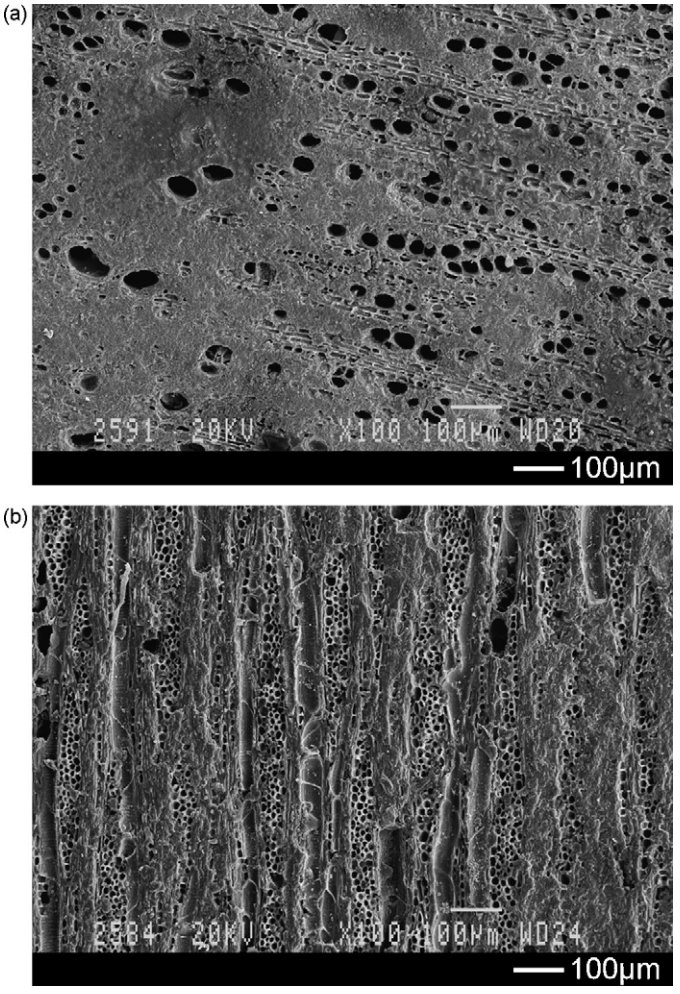

Fig. 5. SEM micrographs of biomorphic SiC derived from almond wood infiltrated in (a) radial section and (b) axial section.

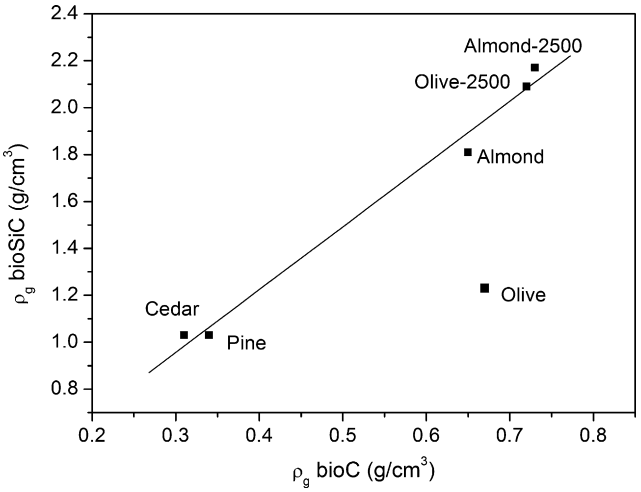

Fig. 6. Linear relationship obtained between biomorphic SiC geometrical density ($\rho_g$bioSiC) and carbon substrate geometrical density ($\rho_g$bioC).

a relatively monomodal pore size distribution parallel to the axial direction. On the other hand, bioSiC derived from almond wood (Fig. 5) exhibits a denser microstructure with a kind of bimodal pore size distribution[10] formed by large open pores parallel to the axial direction (Fig. 5a) and smaller ones parallel to the radial direction (Fig. 5b).

3.2.3. Density and porosity

According to the highly connected porous microstructure observed in SEM micrographs, bioSiC must be a lightweight ceramic material. Table 2 shows the density and porosity values measured for bioSiCs obtained by axial infiltration. It also includes the density of monocrystalline SiC and Si and the true He density of the obtained carbon preforms for comparison. BioSiCs density values range from 1.0 to 1.8 g/cm^3 and total porosity covers the 27–61 vol% range. Total porosity of the bioSiC was defined as the addition of the measured open and closed porosities. The geometrical density that crystalline SiC would have if its porosity were equivalent to that of the bioSiC obtained was calculated and compared with the experimental values. It can be observed that bioSiC geometrical density is lower than the theoretical one, around 20% lower in all cases except for ceramic derived from olive wood which is 37% lower. This fact reveals the existence of lighter elements such as carbon and silicon inside the bioSiC structures and agrees with XRD results where Si peaks were present in all diffractograms. The low density obtained for bioSiC derived from olive wood can be explained by the high closed porosity content of the bioSiC and the low open porosity fraction of the carbon template that results in partial infiltration due to poor access to the liquid silicon.[23]

Despite the different pore structure of each substrate observed by SEM, bioSiCs density is proportional to bioCs density to be infiltrated[20] as shown in Fig. 6. BioSiC derived from olive does not fit in the trend due to the incomplete infiltration-reaction.

Table 3
Mechanical and thermal properties of bioSiC infiltrated in axial direction

	BS (MPa)	ε (%)	E (GPa)	CTE (10^{-6}/°C)
Pine	10	0.19	5	3.44
Cedar	31	0.50	6	3.38
Almond	130	0.50	32	3.04
Olive	43	0.19	23	2.92
SiC				4.3
Si				2.5

BS: bending strength, ε: strain-to-failure, E: Young's modulus, CTE: coefficient of thermal expansion.

3.2.4. Thermal and mechanical properties

Table 3 summarizes thermal and mechanical properties determined for ceramic materials infiltrated in axial direction. CTE values measured for bioSiCs are smaller than for monocrystalline SiC. This measurement also further proves that bioSiCs contain other materials such as silicon and carbon with lower CTE values, as shown by density and XRD results.

Mechanical properties (bending strength, strain-to-failure and Young's modulus) of bioSiCs were determined using three-point bending tests at room temperature. The fracture surfaces of the bioSiCs were found to be flat and smooth, characteristic of brittle fracture.[18] This brittle behaviour agrees with the low strain-to-failure values obtained. Low bending strength values were also measured, except for bioSiC derived from almond wood. Poor mechanical properties of bioSiCs derived from pine and cedar are consequence of the high porosity volume (60%). The partial infiltration of the carbon biotemplate must be the responsible for the low strength of bioSiC derived from olive since closed porosity and unreacted carbon zones are the main

Table 2
Density and porosity values of bioSiC derived from bioC-1400 and infiltrated in axial direction

	ρ_g (g/cm^3)	ρ_s (g/cm^3)	P_{closed} (%)	P_{open} (%)	P_{total} (%)	$\rho_{theoreticalSiC}$ (g/cm^3)
Pine	1.03	2.49	35	24	59	1.30
Cedar	1.03	2.65	17	44	61	1.23
Almond	1.81	2.47	15	12	27	2.30
Olive	1.23	1.97	25	13	38	1.95
SiC[a]		3.21				
Si[a]		2.33				
BioC[b]		1.42 ± 0.2				

ρ_g: geometrical density, ρ_s: powder helium density, P_{closed}: closed porosity volume fraction, P_{open}: open porosity volume fraction, P_{total}: total porosity volume fraction, $\rho_{theoreticalSiC}$: density of SiC containing the same total porosity fraction as bioSiC.

[a] Monocrystalline.

[b] Average He density of the carbon performs.

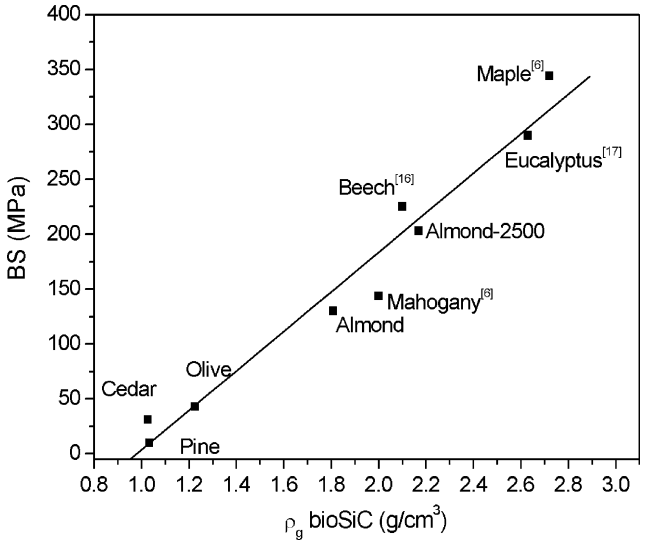

Fig. 7. Linear relationship between three-point bending strength (BS) values measured at room temperature and biomorphic SiC geometrical density ($\rho_g$bioSiC). It also includes data taken from other authors.

nucleation areas for cracks.[6] In the case of bioSiC derived from almond wood, bending strength was 130 MPa, with a density of only 1.8 g/cm^3. This value is higher than those reported by other authors[3,6,8,10,15,16,18,20] for biomorphic SiC materials with similar density.

3.2.5. Correlation of bending strength to density

Bending strength values of bioSiCs measured at ambient temperature are plotted as a function of density in Fig. 7. Biomorphic SiC composites processed by the same technique using mahogany,[6] maple,[6] beech[17] and eucalyptus[18] are included for the sake of comparison. All data points fit a linear relationship in the whole range of bioSiC density produced from wood. This result highlights the strong dependence of bending strength with bioSiC density (inversely, pore volume fraction) not reported before. Previous publications have reported linear correlation of elastic modulus[6] and compressive strength[10,17,20] versus density, but high scatter of results have been found for bending strength[16,17,24] and fracture toughness.[6,24] Results presented here show that bending strength values of bioSiCs derived from wood are mainly determined by the bioSiC density, the contribution of pore structure factor not being so decisive. BioSiC density and hence wood density can be used as good approach for the prediction of bioSiC bending strength.

Several authors have attempted to model the mechanical properties of these materials. However, poor agreement is usually found between the models and the measured values, this being commonly attributed to the deviation of tested materials from the idealized structure.[20,23]

Regarding the different pore structure of bioceramics derived from softwood and hardwood, usually two different approaches are used. For bioceramics derived from softwood (over 70% porosity and relatively uniform pore size distribution) the solid cellular model of Gibson and Ashby[25] is used, where strength is mostly related to the bending strength of the cell walls.[8,20,26] For bioceramics derived from hardwood (lower porosity and non-uniform pore size distribution) the theory developed by Rice[27] is used, where the strength depends on the minimum solid area (MSA) perpendicular to the applied stress.[10,15,16,23]

The features of bioSiC studied in this work are closer to porous materials than to cellular solids. Therefore, it seems more realistic to use the approach of minimum solid area. This model describes relative strength as an exponential function of the pore volume fraction over a wide range of porosities.

$$\frac{\sigma}{\sigma_o} = e^{-bP} \quad (1)$$

where σ is the strength of the porous material, σ_o is the strength of the completely dense material, P is the pore volume fraction and b is a constant often found to be equal to 5 for spherical pores and higher values for elongated pores.[16] Total porosity can be expressed as inverse of fractional density (ratio of geometrical density of porous material ρ_g over density of powder material ρ_s).

$$P = 1 - \frac{\rho_g}{\rho_s} \quad (2)$$

and the following linear expression is obtained when substituting Eq. (2) into Eq. (1) and applying logarithm

$$\ln \sigma = \ln \sigma_o - b\left(1 - \frac{\rho_g}{\rho_s}\right) \quad (3)$$

Fig. 8 plots the fitting of experimental data to Eq. (3) from which the following model parameters were deduced: $b = 8$, $\sigma_o = 1375$ MPa and a correlation factor of $R^2 = 0.99$. Greil et al.[16] have also reported good agreement between bending strength experimental values and MSA model but with a value of the constant ($b = 4$ in axial direction) lower than the predicted by the model. Despite the evident microstructural peculiarities of each precursor, fairly good agreement to straight line is observed for all data except for cedar. This fact implies that bending strength is mainly controlled by the amount of porosity remaining in the material after infiltration.

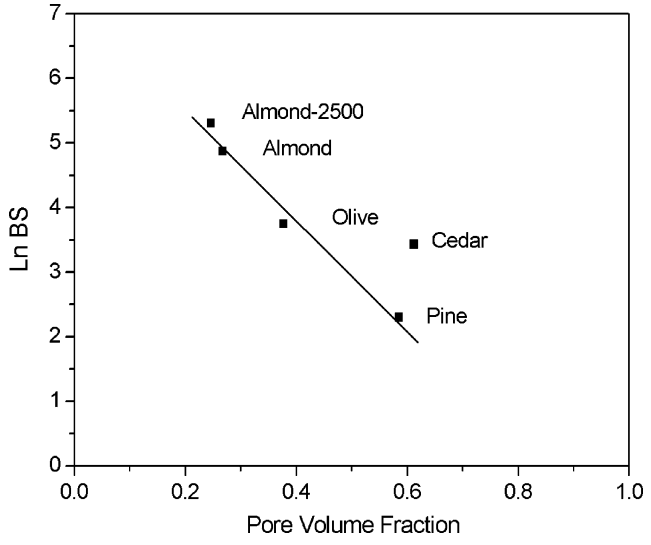

Fig. 8. Plot of Neperian logarithms of bending strength values versus pore volume fraction ($1 - \rho_g/\rho_s$) of bioSiC. Data fitted by the MSA model (see Eq. (3)).

Table 4
Density, porosity, mechanical and thermal properties of the bioSiC derived from bioC-2500 and infiltrated in axial direction

	ρ_g (g/cm^3)	ρ_s (g/cm^3)	P_{closed} (%)	P_{open} (%)	BS (MPa)	ε (%)	E (GPa)	CTE (10^{-6}/°C)
Almond	2.17	2.82	14	9	203	0.35	54	3.56
Olive	2.09	2.74	15	8	17	0.12	14	3.64

ρ_g: geometrical density, ρ_s: powder helium density, P_{closed}: closed porosity volume fraction, P_{open}: open porosity volume fraction, BS: bending strength, ε: strain-to-failure, E: Young's modulus, CTE: coefficient of thermal expansion.

3.2.6. Effect of high temperature treatment

As shown above, bending strength of bioSiC strongly depends on bioSiC density which is proportional to bioC density (Fig. 6). In order to increase bioC density two different approaches can be used: selection of a denser carbon precursor (Fig. 2) or increase the density of the bioC by heat treatment at higher temperature. Heat treatment of bioC at higher temperature modifies the shape and size of pores since there is a partial graphitization of the carbon structure.[7,21] No previous report of the effect of this treatment on bioSiC properties has been described in literature.

Hence, some carbon biotemplates obtained after pyrolysis and carbonization at 1400 °C were further heated up to 2500 °C in an argon flow (bioC-2500). The selected precursors were almond and olive woods, which exhibited the highest densities. Density and porosity values of bioC-2500 are given in Table 1. Density of bioC-2500 increased around 10% for both precursors compared to bioC-1400. Open porosity fraction of almond precursor decreased 30% while closed porosity fraction increased slightly, resulting in a total porosity decrease of 10%. In contrast, the porosity of bioC-2500 from olive increased 6% mainly closed porosity.

BioC-2500 was infiltrated with liquid silicon in the axial direction as preferred direction for reactive infiltration. XRD spectra of reaction products were analogous to Fig. 3a where large β-SiC peaks were observed together with some residual Si. BioSiCs produced from bioC-2500 were characterized in the same way as bioC-1400 and results are summarized in Table 4, the density following the tendency found for bioSiCs produced from bioC-1400 (Fig. 6). BioC-2500 derived from almond wood produced bioSiC with 20% higher density and 15% lower total porosity in respect to bioSiC produced from bioC-1400. Bending strength values obtained, in majority of the tests, were above 200 MPa, giving an average value of 203 MPa for a density of only 2.17 g/cm^3. These results match the relationship obtained before (Figs. 7 and 8), as predicted. This bending strength value is also higher than any other reported for lignocelllulosic materials[16,19] and in the range of commercial reaction-bonded-silicon-carbide (RBSC) produced from others carbon-rich precursors such as coke. The improvement in mechanical properties is attributed to the increase in density of bioSiC produced. Increase in bioSiC density is an evidence of higher SiC conversion due to higher reactivity of bioC-2500 than bioC-1400 with liquid Si to produce bioSiC. SiC formation is controlled by the structural organization of the carbon substrate, showing higher reactivity the more organized carbon material, forming a more cohesive strongly connected SiC network.[28] On the other hand, bioSiC produced from bioC-2500 derived from olive wood experienced a density increase of 70%, total porosity decreasing 40% in respect to bioSiC obtained from bioC-1400.

4. Conclusions

Carbon preforms derived from four Mediterranean types of wood were used as template for fabrication of bioSiC by reactive infiltration with liquid silicon. The main conclusions of this work are as follows:

Infiltration in axial direction showed a higher SiC conversion due to easier transport of liquid silicon through the channels of the carbon preform.
In general, bioSiC produced is lightweight, it retains the microstructure of the original wood and it is highly porous and anisotropic. The diversity on wood structures lead to ceramics with a wide range of density and pore morphologies.
BioSiC bending strength values mainly depend on bioSiC density.
BioSiC ceramic properties are affected by the maximum temperature of the heat treatment of the carbon structure.
Carbons heat-treated at higher temperature exhibit higher density, a more organized carbon structure that increases reactivity with Si to form bioSiC with enhancement in mechanical properties.
BioSiC derived from almond carbon treated at 2500 °C exhibited mechanical properties in the range of commercial RBSC.

Acknowledgments

This work was partially supported by European Community project ALICE (G3RD-CT-2002-00799) and Spanish MYCT (grant MAT 2004-03139). N.R. Calderon is grateful to Spanish MEC (predoctoral grant FPU-AP-2004-2907). Schunk Kohlenstofftechnik GmbH is also acknowledged for carrying out the high temperature treatment.

References

1. Sieber, H., Biomimetic synthesis of ceramics and ceramic composites. *Mater. Sci. Eng. A: Struct.*, 2005, **412**, 43–47.
2. Greil, P., Biomorphous ceramics from lignocellulosics. *J. Eur. Ceram. Soc.*, 2001, **21**, 105–118.
3. Arellano-Lopez, A. R., Martinez-Fernandez, J., Gonzalez, P., Dominguez, C., Fernandez-Quero, V. and Singh, M., Biomorphic SiC: a new engineering ceramic material. *Int. J. Appl. Ceram. Technol.*, 2004, **1**, 56–67.
4. Gonzalez, P., Serra, J., Liste, S., Chiussi, S., Leon, B., Perez-Amor, M., Martinez-Fernandez, J., Arellano-Lopez, A. R. and Varela-Feria, F. M.,

New biomorphic SiC ceramics coated with bioactive glass for biomedical applications. *Biomaterials*, 2003, **24**, 4827–4832.
5. Greil, P., Advanced engineering ceramics. *Adv. Eng. Mater.*, 2002, **4**, 247–254.
6. Singh, M. and Salem, J. A., Mechanical properties and microstructure of biomorphic silicon carbide ceramics fabricated from wood precursors. *J. Eur. Ceram. Soc.*, 2002, **22**, 2709–2717.
7. Singh, M. and Yee, B. M., Reactive processing of environmentally conscious, biomorphic ceramics from natural wood precursors. *J. Eur. Ceram. Soc.*, 2004, **24**, 209–217.
8. Martinez-Fernandez, J., Valera-Feria, F. M. and Singh, M., High temperature compressive mechanical behavior of biomorphic silicon carbide ceramics. *Scripta Mater.*, 2000, **43**, 813–818.
9. Greil, P., Lifka, T. and Kaindl, A., Biomorphic cellular silicon carbide ceramics from wood. I. Processing and microstructure. *J. Eur. Ceram. Soc.*, 1998, **18**, 1961–1973.
10. Fernandez, J. M., Munoz, A., Lopez, A. R. D., Feria, F. M. V., Dominguez-Rodriguez, A. and Singh, M., Microstructure-mechanical properties correlation in siliconized silicon carbide ceramics. *Acta Mater.*, 2003, **51**, 3259–3275.
11. Vogli, E., Mukerji, J., Hoffman, C., Kladny, R., Sieber, H. and Greil, P., Conversion of oak to cellular silicon carbide ceramic by gas-phase reaction with silicon monoxide. *J. Am. Ceram. Soc.*, 2001, **84**, 1236–1240.
12. Qian, J. M., Wang, J. P., Jin, Z. H. and Preparation, Properties of porous microcellular SiC ceramics by reactive infiltration of Si vapor into carbonized basswood. *Mater. Chem. Phys.*, 2003, **82**, 648–653.
13. Vogli, E., Sieber, H. and Greil, P., Biomorphic SiC-ceramic prepared by Si-vapor phase infiltration of wood. *J. Eur. Ceram. Soc.*, 2002, **22**, 2663–2668.
14. Qian, J. M., Wang, J. P., Qiao, G. J. and Jin, Z. H., Preparation of porous SiC ceramic with a woodlike microstructure by Sol–Gel and carbothermal reduction processing. *J. Eur. Ceram. Soc.*, 2004, **24**, 3251–3259.
15. Arellano-Lopez, A. R., Martinez-Fernandez, J., Varela-Feria, F. M., Orlova, T. S., Goretta, K. C., Gutierrez-Mora, F., Chen, N. and Routbort, J. L., Erosion and strength degradation of biomorphic SiC. *J. Eur. Ceram. Soc.*, 2004, **24**, 861–870.
16. Greil, P., Lifka, T. and Kaindl, A., Biomorphic cellular silicon carbide ceramics from wood. II. Mechanical properties. *J. Eur. Ceram. Soc.*, 1998, **18**, 1975–1983.
17. Presas, M., Pastor, J. Y., Llorca, J., Arellano-Lopez, A. R., Martinez-Fernandez, J. and Sepulveda, R. E., Mechanical behavior of biomorphic Si/SiC porous composites. *Scripta Mater.*, 2005, **53**, 1175–1180.
18. Presas, M., Pastor, J. Y., Llorca, J., Lopez, A. R. A., Fernandez, J. M., Sepulveda, R. and Microstructure, Fracture properties of biomorphic SiC. *Int. J. Refract. Met. H*, 2006, **24**, 49–54.
19. Sieber, H., Hoffmann, C., Kaindl, A. and Greil, P., Biomorphic cellular ceramics. *Adv. Eng. Mater.*, 2000, **2**, 105–109.
20. Varela-Feria, F. M., Martinez-Fernandez, J., Arellano-Lopez, A. R. and Singh, M., Low density biomorphic silicon carbide: microstructure and mechanical properties. *J. Eur. Ceram. Soc.*, 2002, **22**, 2719–2725.
21. Byrne, C. E. and Nagle, D. C., Carbonized wood monoliths—characterization. *Carbon*, 1997, **35**, 267–273.
22. Byrne, C. E. and Nagle, D. C., Carbonization of wood for advanced materials applications. *Carbon*, 1997, **35**, 259–266.
23. Kaul, V. S., Faber, K. T., Sepulveda, R., Lopez, A. R. D. and Martinez-Fernandez, J., Precursor selection and its role in the mechanical properties of porous SiC derived from wood. *Mater. Sci. Eng. A: Struct.*, 2006, **428**, 225–232.
24. Qiao, G. J., Ma, R., Cai, N., Zhang, C. G. and Jin, Z. H., Mechanical properties and microstructure of Si/SiC materials derived from native wood. *Mater. Sci. Eng. A: Struct.*, 2002, **323**, 301–305.
25. Gibson, L. J. and Ashby, M. F., *Cellular Solids: Structure and Properties*. Cambridge University Press, Cambridge, 1999.
26. Greil, P., Vogli, E., Fey, T., Bezold, A., Popovska, N., Gerhard, H. and Sieber, H., Effect of microstructure on the fracture behavior of biomorphous silicon carbide ceramics. *J. Eur. Ceram. Soc.*, 2002, **22**, 2697–2707.
27. Rice, R. W., *Porosity of Ceramics*. M. Dekker, New York, 1998.
28. Narciso-Romero, F. J., Rodriguez-Reinoso, F. and Diez, M. A., Influence of the carbon material on the synthesis of silicon carbide. *Carbon*, 1999, **37**, 1771–1778.